Supporting Information

Biodegradable Manganese-Doped Calcium Phosphate Nanotheranostics for Traceable Cascade Reaction-Enhanced Anti-Tumor Therapy

Lian-Hua Fu,[†,⊥,§] *Yan-Ru Hu,*[†,§], *Chao Qi,*[†] *Ting He,*[†] *Shanshan Jiang,*[†] *Chao Jiang,*[†] *Jin He,*[†] *Junle Qu,*[⊥] *Jing Lin,*[†] *and Peng Huang*[†,*]

[†]Marshall Laboratory of Biomedical Engineering, International Cancer Center, Laboratory of Evolutionary Theranostics (LET), School of Biomedical Engineering, Shenzhen University Health Science Center, Shenzhen 518060, China

[⊥]Key Laboratory of Optoelectronic Devices and Systems of Ministry of Education and Guangdong Province, College of Optoelectronic Engineering, Shenzhen University, Shenzhen 518060, China

E-mail: peng.huang@szu.edu.cn

[§]These authors contribute equally.

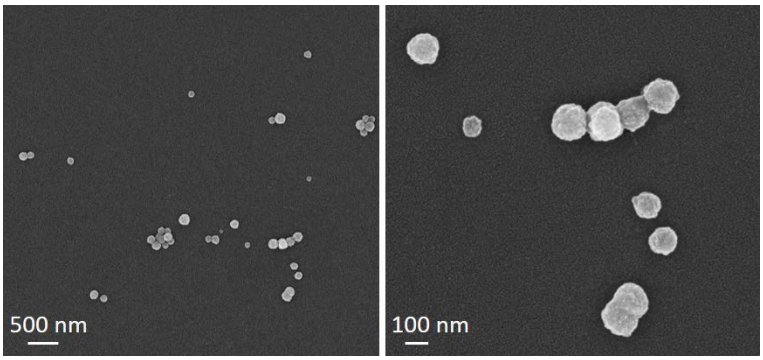

Figure S1. SEM images of GOx-MnCaP.

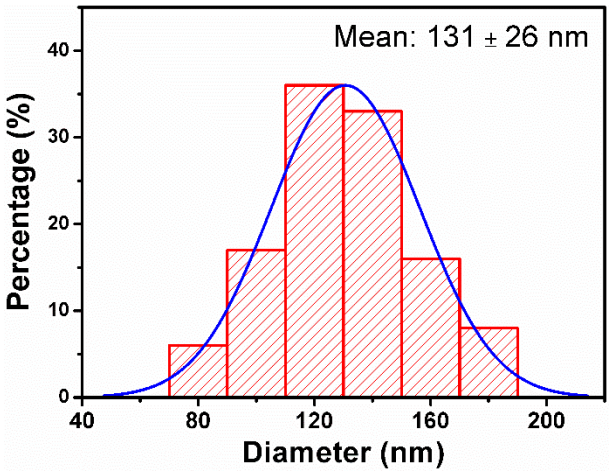

Figure S2. Size distribution of GOx-MnCaP analysized by Image J software (NIH, USA).

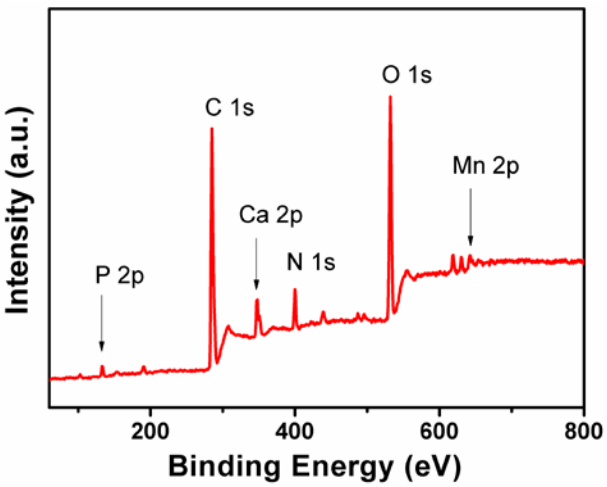

Figure S3. XPS spectrum of GOx-MnCaP. The C 1s, N 1s, O 1s, Mn 2p, Ca 2p, and P 2p are found in the spectrum, which is consist with the results of elemental mapping analysis (Figure 1b).

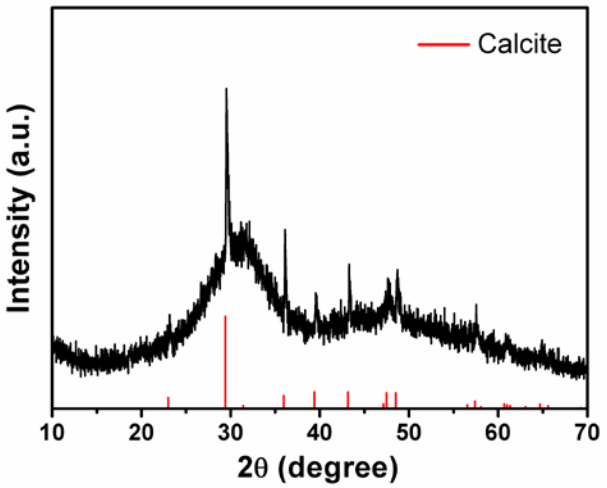

Figure S4. XRD pattern of GOx-MnCaP. The broad peak at around 2θ = 30° indicating an amorphous phase of CaP, while the other peaks are attributed to calcite ($CaCO_3$) (JCPDS 05-0586), an anhydrous phase of calcium carbonate.

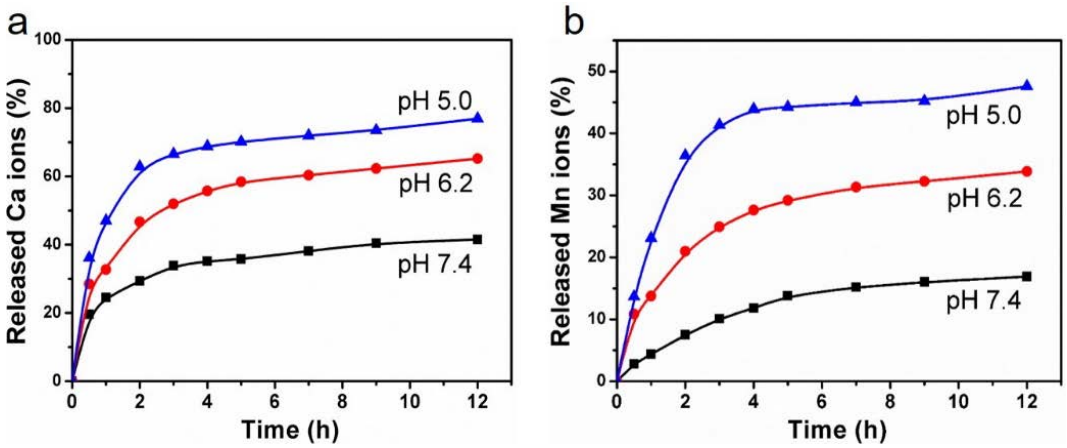

Figure S5. (a) Ca^{2+} and (b) Mn^{2+} release from GOx-MnCaP in PBS with different pH values.

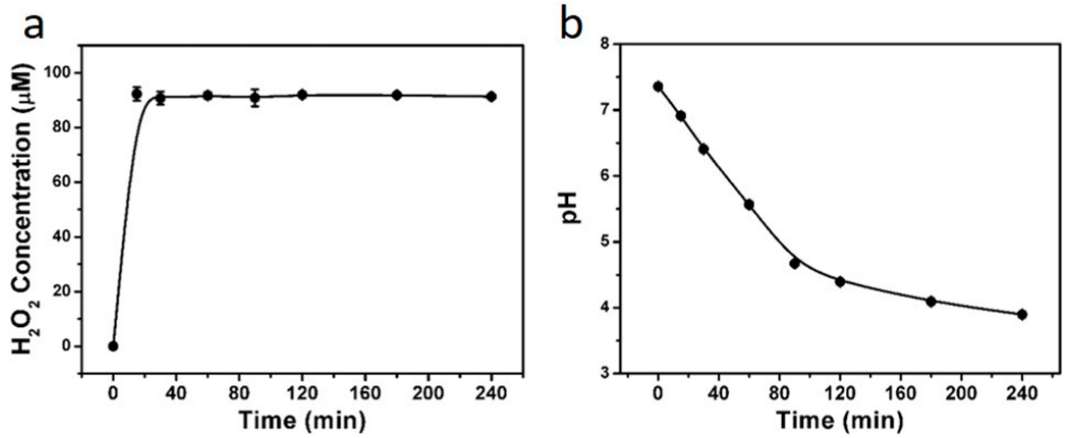

Figure S6. (a) The concentration of generated H_2O_2 and (b) pH values at different time points arising from the GOx-MnCaP catalyzed decomposition reaction of glucose (1000 μg mL^{-1}).

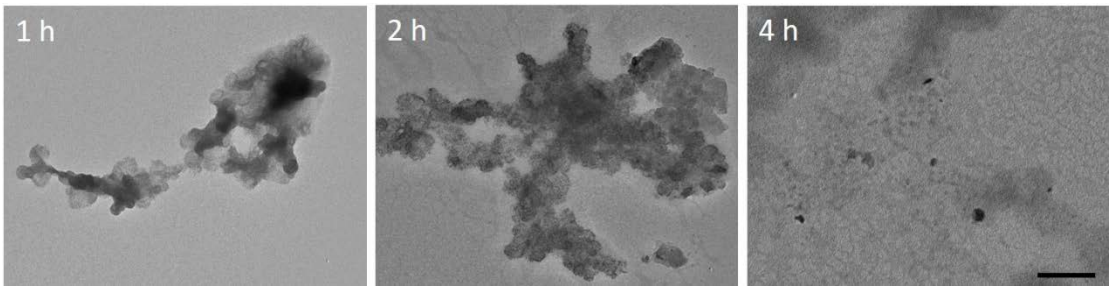

Figure S7. TEM images of GOx-MnCaP incubated with glucose (1000 μg mL^{-1}) for different time points. Scale bar: 500 nm.

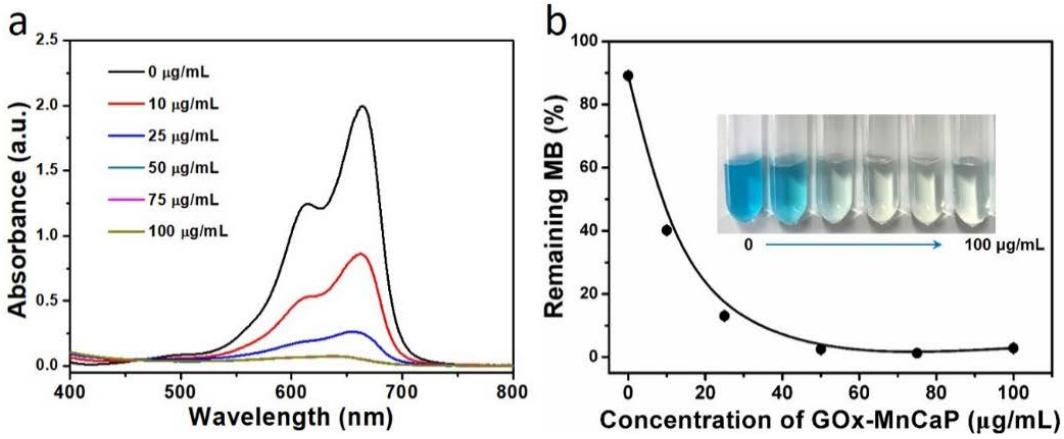

Figure S8. (a) UV/Vis spectra and (b) MB degradation and photo (inset) by GOx-MnCaP mediated Fenton-like reaction with different concentration of GOx-MnCaP for 3 h. [H_2O_2] = 10 mM. The MB degradation increases with increasing of GOx-MnCaP concentration, and MB could be almost completely degraded at a low GOx-MnCaP concentration of 50 μg mL^{-1}.

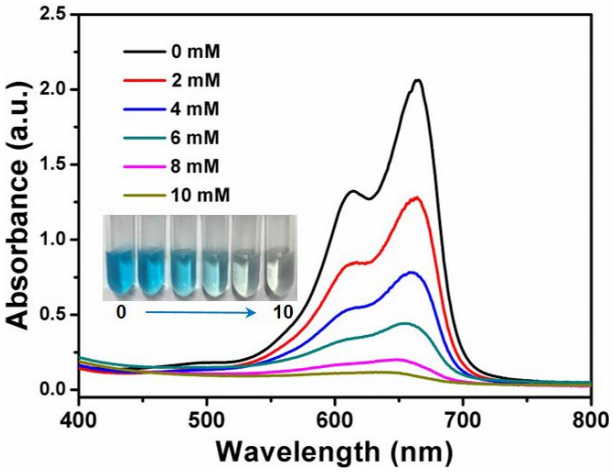

Figure S9. UV/Vis spectra and photo (inset) of MB aqueous solution by GOx-MnCaP mediated Fenton-like reaction with different concentration of H_2O_2 for 3 h. The MB degradation increases with increasing H_2O_2 concentration. [GOx-MnCaP] = 100 μg mL^{-1}

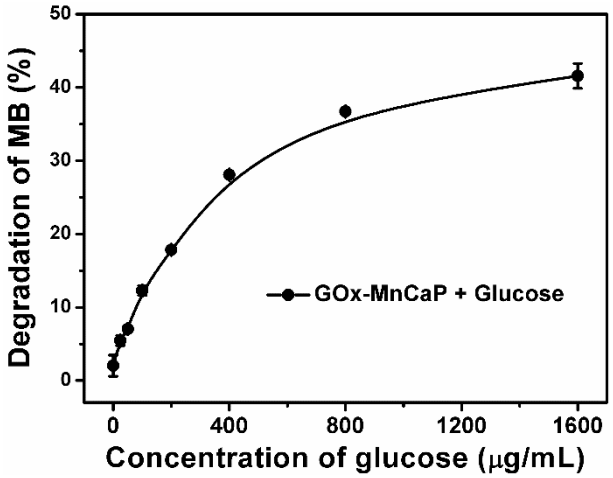

Figure S10. MB degradation by GOx-MnCaP mediated Fenton-like reaction between Mn^{2+} and the H_2O_2 generated from the catalytic reaction of GOx and glucose. [GOx-MnCaP] = 100 μg mL^{-1}, [H_2O_2] = 0 mM.

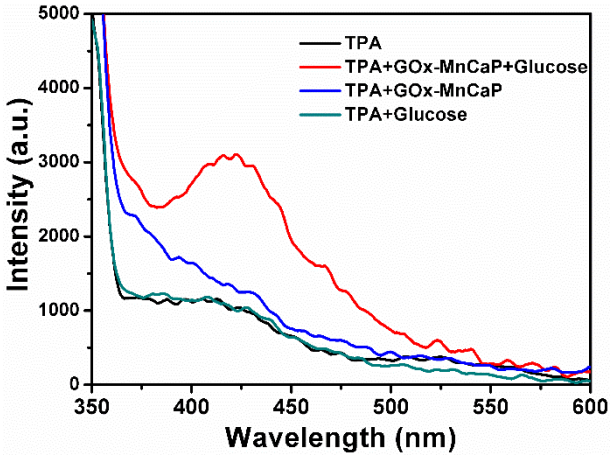

Figure S11. Fluorescence spectra of TPA-OH for detection of •OH generated by GOx-MnCaP mediated Fenton-like reaction between released Mn^{2+} and the H_2O_2 generated from the GOx-triggered glucose oxidation. [GOx-MnCaP] = 100 μg mL^{-1}, [H_2O_2] = 0 mM, [glucose] = 800 μg mL^{-1}.

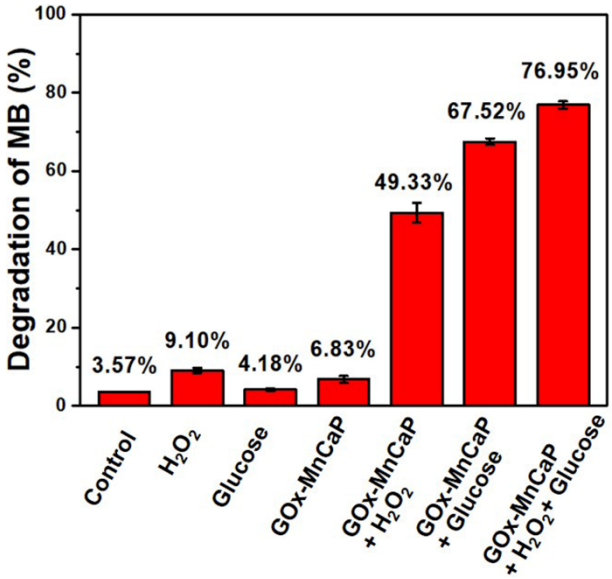

Figure S12. The degradation percent of MB after different treatments for 7 h (mean ± SD, n = 3). Control group: MB alone, other groups: [GOx-MnCaP] = 100 μg mL^{-1}, [H_2O_2] = 2 mM, [glucose] = 1000 μg mL^{-1}.

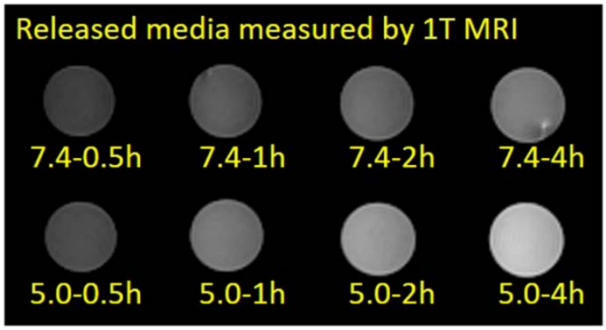

Figure S13. T_1-weighted MR images of GOx-MnCaP released PBS media measured by 1T-MRI. GOx-MnCaP showed an apparent time-dependent brightening effect at pH 5.0, while a rather weak signal was observed at pH 7.4.

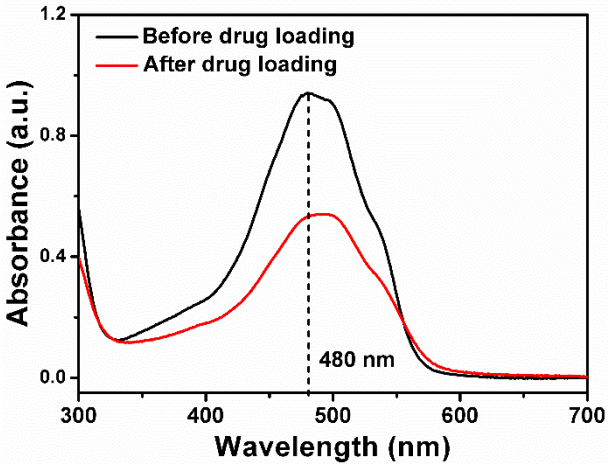

Figure S14. UV/Vis absorption of DOX solution before and after loading in GOx-MnCaP suspension. Each solution was diluted 20 times. The drug loading efficiency was calculated to 43.43% based on the adsorption of 480 nm according to the following equation: Loading efficiency = ((total DOX – unloaded DOX) / total DOX) × 100%.

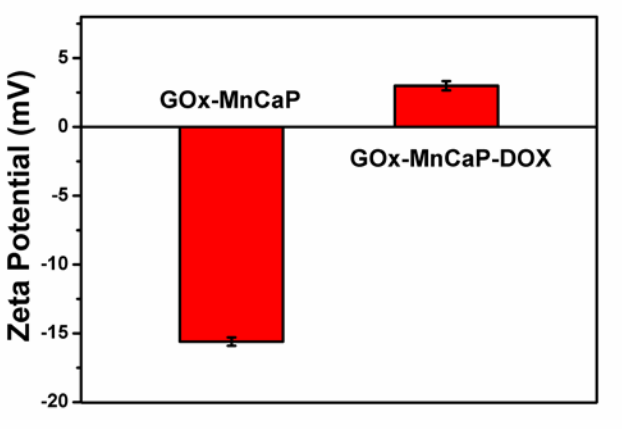

Figure S15. Zeta potential of GOx-MnCaP and GOx-MnCaP-DOX in water.

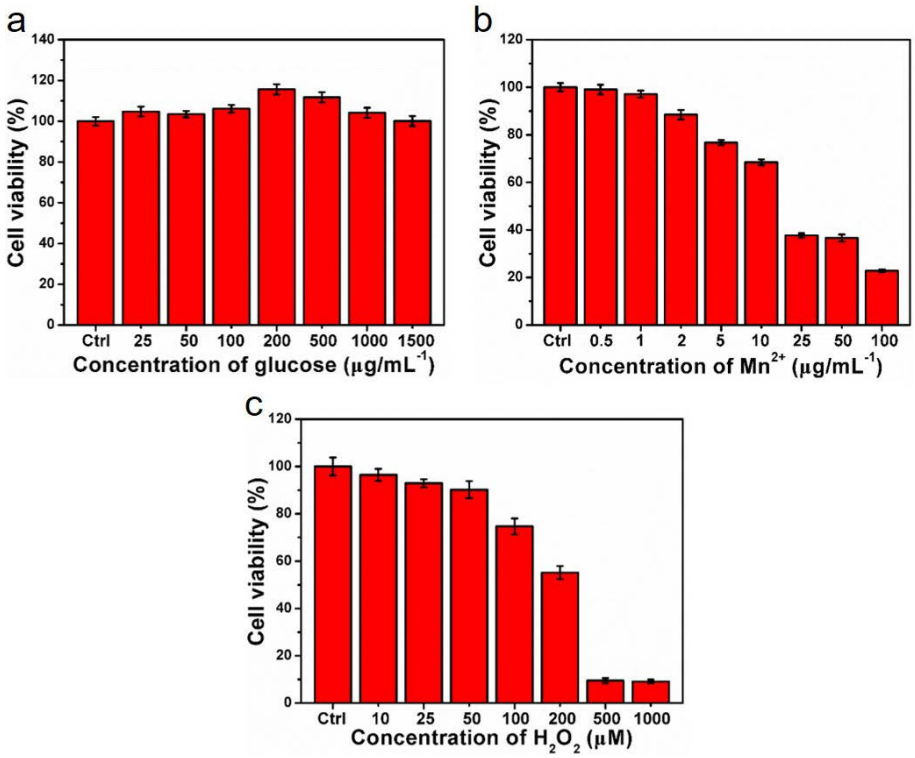

Figure S16. The viabilities of 4T1 cells incubated with (a) different concentrations of glucose, (b) $MnCl_2$ at different Mn concentrations, and (c) different concentrations of H_2O_2 for 24 h.

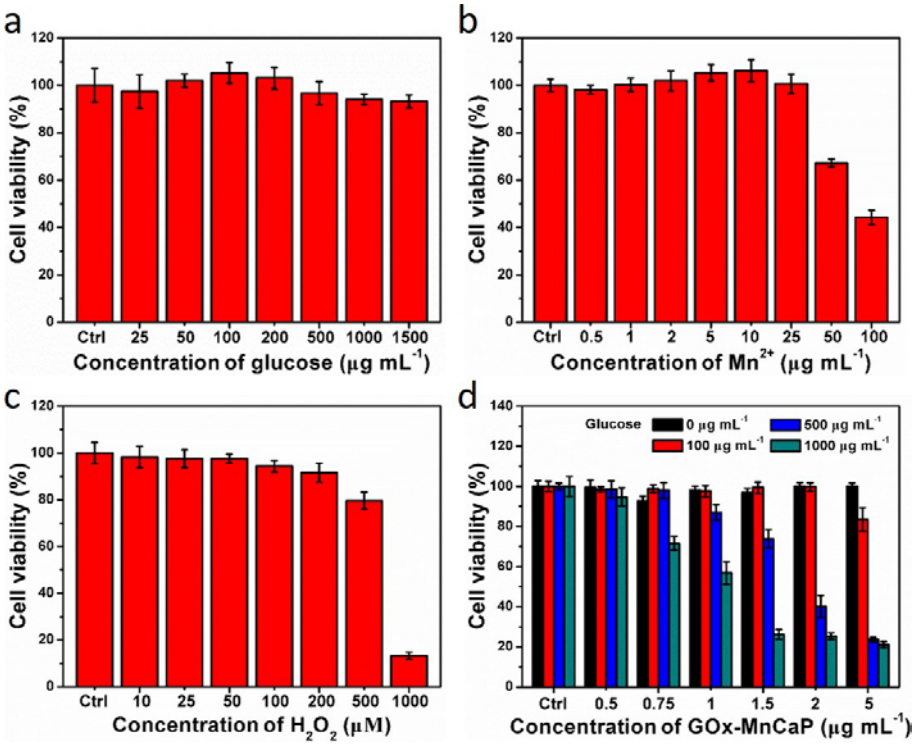

Figure S17. The viabilities of U87MG cells incubated with (a) different concentrations of glucose, (b) $MnCl_2$ at different Mn concentrations, and (c) different concentrations of H_2O_2 for 24 h. (d) The viabilities of U87MG cells incubated with GOx-MnCaP in different concentrations of glucose-containing DMEM media.

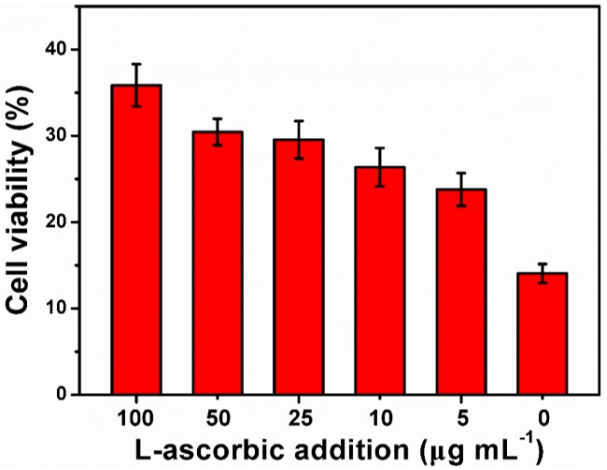

Figure S18. L-ascorbic acid-assisted cell rescue profiles of 4T1 cells' cytotoxicity induced by GOx-MnCaP in glucose-containing DMEM media.

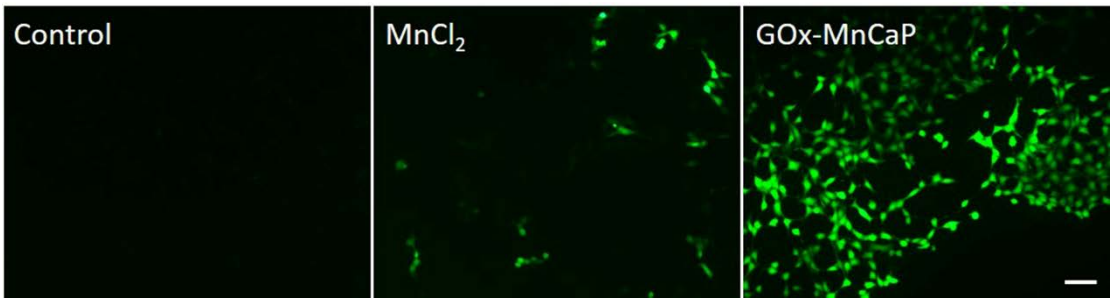

Figure S19. Microscopy images of 4T1 cells after incubation with fresh medium, $MnCl_2$, and GOx-MnCaP for 2 h, and stained with ROS fluorescene probe DCFH-DA. Scale bar: 200 μm.

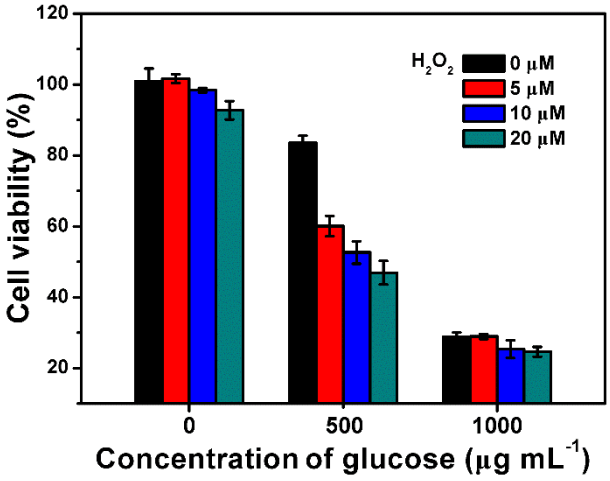

Figure S20. The viabilities of 4T1 cells after incubation with GOx-MnCaP with different concentrations of H_2O_2 in glucose-containing DMEM media.

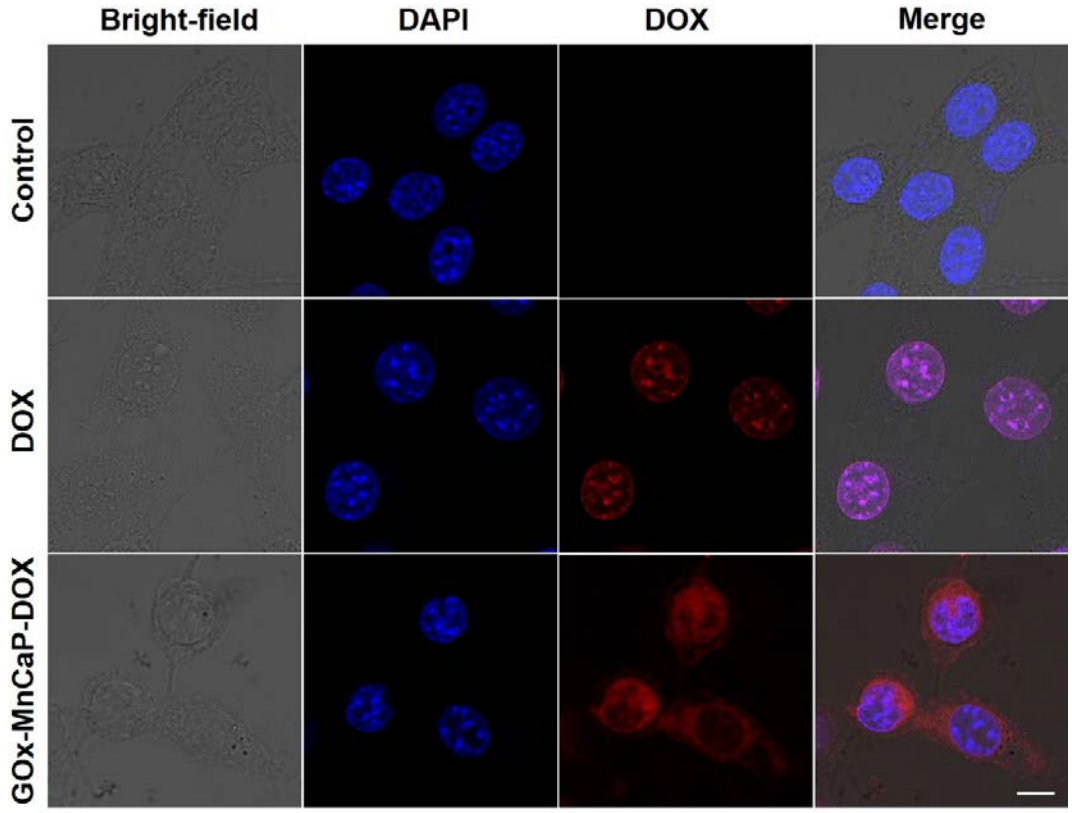

Figure S21. Confocal laser scanning microscopic (CLSM) images of 4T1 cells after co-incubation with GOx-MnCaP-DOX or free DOX for 2 h. Scale bar: 10 μm. Blue fluorescence: DAPI, red fluorescence: DOX.

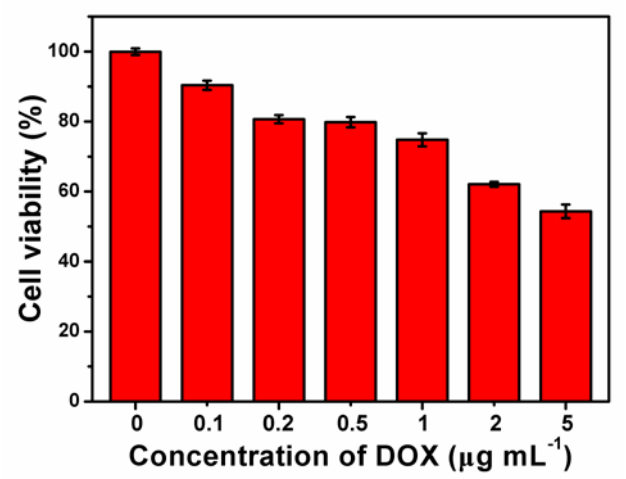

Figure S22. The viabilities of 4T1 cells after incubated with DOX at different concentrations.

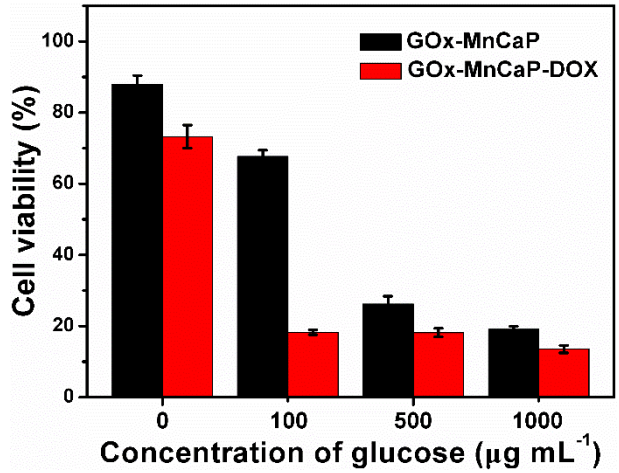

Figure S23. The viabilities of 4T1 cells after incubation with different samples at the equivalent concentration of 5 μg mL^{-1} GOx-MnCaP in glucose-containing DMEM media.

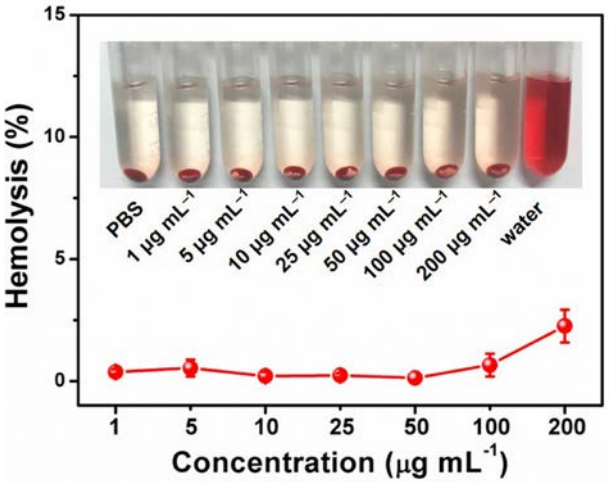

Figure S24. Hemolysis analysis of GOx-MnCaP suspension at various concentrations (mean ± SD, n = 3). Deionized water and PBS were used as positive and negative controls, respectively. The results showed that the hemolysis rates of different concentrations (1–200 μg mL^{-1}) of GOx-MnCaP were almost lower than 2.26%.

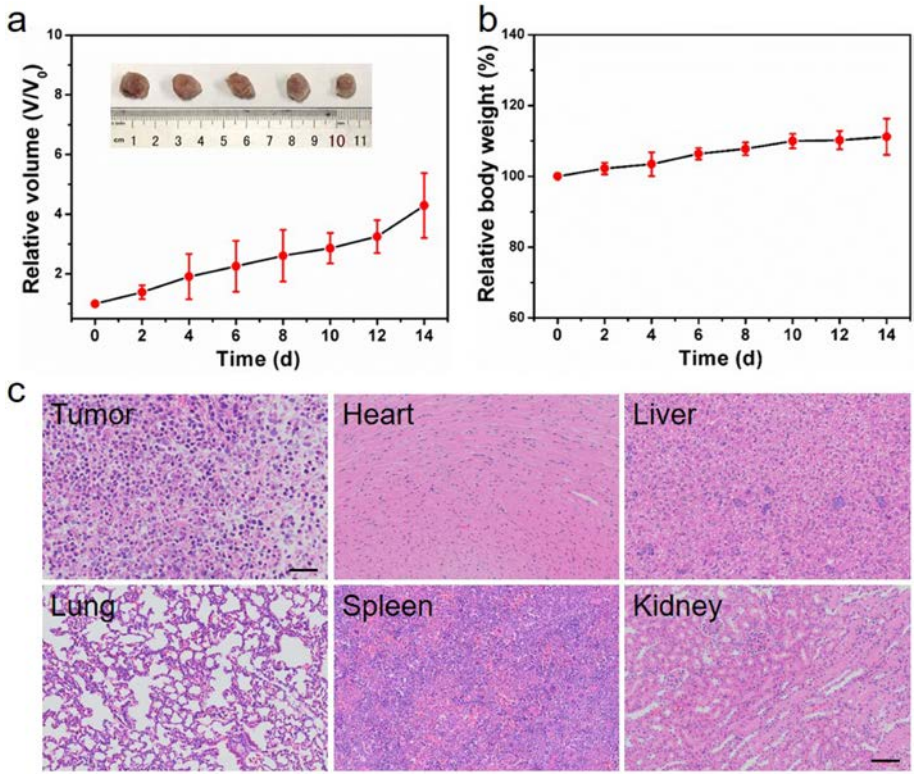

Figure S25. (a) Tumor growth curve of 4T1 tumor-bearing mice treated by DOX. n = 5. Inset, digital photos of excised tumors from the mice after 14 days of treatment. (b) Average body weight variation of the mice during the treatment. (c) H&E staining images of dissected tumor tissue (scale bar, 50 μm) and major organs (scale bar, 100 μm) from 4T1 tumor-bearing mice after 14 days of treatment.

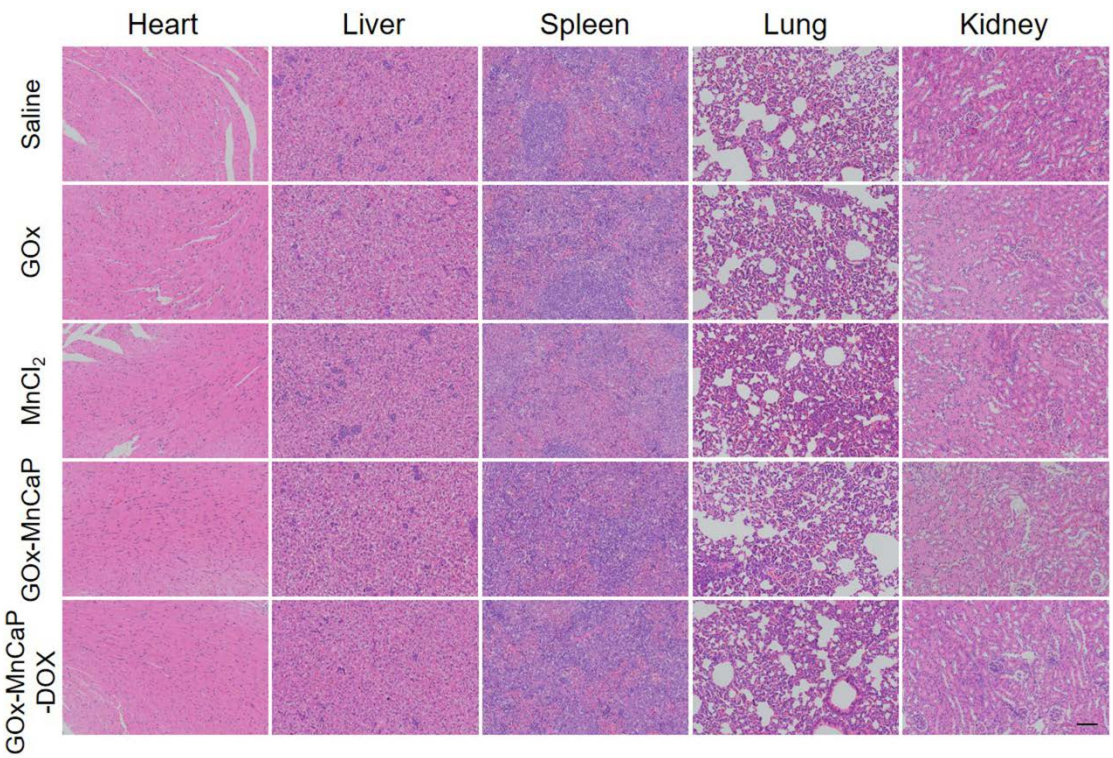

Figure S26. H&E staining images of dissected major organs of mice on day 14 after intratumoral injection of saline, GOx, $MnCl_2$, GOx-MnCaP, and GOx-MnCaP-DOX, respectively. Scale bar: 100 μm.